Front. Earth Sci.
DOI 10.1007/s11707-015-0523-6

RESEARCH ARTICLE

Variation and future trends in precipitation over summer and autumn across the Yunnan region

Ziniu XIAO (✉)[1], Xiuhua ZHOU[2], Ping YANG[3], Hua LIU[3]

1 State Key Laboratory of Numerical Modeling for Atmospheric Sciences and Geophysical Fluid Dynamics, Institute of Atmospheric Physics, Chinese Academy of Sciences, Beijing 100029, China
2 Guangxi Climate Center, Nanning 530022, China
3 China Meteorological Administration Training Center, Beijing 100081, China

Abstract This study analyzed the changes in precipitation over summer and autumn across the Yunnan region of China, and undertook a composite analysis of the atmospheric circulations in the troposphere, which included an analysis of the interannual and interdecadal variations. This paper examines in detail the circulation backgrounds of the wet and dry periods in summer and autumn and their correlations with the sea surface temperature. The results indicated that the summer and autumn precipitation across Yunnan has significantly decreased over the past 50 years. Furthermore, since the beginning of the century, the summer and autumn precipitation cycle has been in a low precipitation phase. The overlap of two extremely low rain phases has caused frequent droughts in the region. In addition, the atmospheric circulation fields during these wet and dry periods are very different. These are mainly shown as a meridional wind anomaly in eastern China in the low atmosphere, as a cross-equatorial airflow anomaly, a tropical zonal wind anomaly over the Indian Ocean, and as a related South Asia High and Western Pacific Subtropical High. Further analysis suggested that the SST over the Indian Ocean and the Pacific warm pool critically affect the anomalous summer and autumn precipitation over Yunnan by impacting the monsoon circulations. Future projections for greenhouse gas warming suggest a potential anomalous circulation background between 2010 and 2020 which may result in less precipitation during the wet season or even drought events across the Yunnan region.

Keywords precipitation over Yunnan, circulation background, sea temperature anomaly, future trend

Received May 3, 2014; accepted March 3, 2015

E-mail: xiaozn@lasg.iap.ac.cn

1 Introduction

Global warming predictions suggest that droughts, floods, and other extreme weather events will become more frequent, and that these events will directly impact people's livelihoods and the local economy. As a result, the prediction and identification of the causes of extreme weather events has become essential (Liu et al., 1996; Frich et al., 2002; García-Herrera et al., 2007; Korecha and Barnston, 2007). Extreme successive drought events have occurred over southwest China in recent years, including an abnormal drought over Yunnan in spring 2005, a severe summer drought across Sichuan and Chongqing in summer 2006, and a disastrous drought over the five provinces centered over Yunnan and Guizhou Provinces between autumn 2009 and spring 2010 (Huang et al., 2012). These droughts have brought inestimable economic losses to the affected areas. The severe drought event in southwest China between autumn 2009 and spring 2010 has been investigated and analyzed by a number of researchers (Song et al., 2011; Huang et al., 2012; Qian and Zhang, 2012). The climate in this region is highly variable. These persistent drought events have numerous impactful factors and the related physical mechanisms are complex.

Yunnan, China lies in a low-latitude plateau. It is the convergence zone of two monsoons: the East Asian and South Asian monsoons, and is therefore sensitive to monsoonal variations. The characteristics of a monsoon can vary due to the interaction of many different elements. Several studies have indicated that the Asian monsoons are weakening (Wang, 2001). The weakening of the East Asian monsoon helps to form the flood patterns seen in southern China and the droughts recorded in northern China (Ding et al., 2013; Wang and Fan, 2013). The East Asian summer and winter monsoons have declined since the mid-1970s. The precipitation over the southwest region

has correspondingly changed; that is, the southwestern areas that are affected by the weak East Asian summer monsoon experienced decreased rainfall in summer. Qi et al. (2012) suggested that, because summer precipitation over the southwest accounts for the largest proportion of the total yearly rainfall, the variation in the summer precipitation must directly influence the total yearly precipitation pattern. Therefore, the weakening of the East Asian summer monsoon is an important impact factor which has led to a reduction in annual precipitation over the southwest region. The results also indicated that there was a close relationship between the South Asian summer monsoon and the precipitation over Yunnan Province. Moreover, the South Asian summer monsoon index has also decreased in recent decades (Li et al., 2014).

Many scholars use global atmosphere-ocean coupled models (Min et al., 2004; Zhang et al., 2011; Chen, 2012; Diffenbaugh and Giorgi, 2012; Lau et al., 2012; Liu et al., 2012; Deng et al., 2013) or regional climate models (Boo et al., 2006; Sato et al., 2007) for future climate prediction and projection. These are primarily long-term simulations based on the A2 scenario in the Special Report on Emission Scenarios (SRES; Nakicenovic and Swart, 2000) or Representative Concentration Pathways (RCPs; van Vuuren et al., 2007; Meinshausen et al., 2011; Taylor et al., 2012). Based on the Coupled Model Intercomparison Program 5 (CMIP5) data, Xu and Xu (2012) found that precipitation will tend to decrease in the southern parts of China between 2011 and 2040. In addition, the Northern Hemisphere monsoon onset will advance and withdrawal will be delayed between 2006 and 2100, causing monsoon precipitation to increase significantly (Lee and Wang, 2014).

It is important to determine if such a series of dry years are random weather events, variations in the annual weather cycle, or longer term decadal or inter-decadal changes. This study analyzed the variation characteristics, the atmospheric circulation background, and the potential trigger factors for precipitation in summer (June, July, August) and autumn (September, October, November) across the Yunnan region, investigated if circulations could cause precipitation anomalies in summer and autumn before 2020 by analyzing the CMIP5 data, and estimated the future development trend for drought. Global climate change causes uneven temporal and spatial precipitation distributions, which means that flood and drought disasters would become more frequent. Climate change in Yunnan Province is directly related to critical issues, such as the sustainable regional economic development, water resources utilization, environmental change, impact on human society, etc. Therefore, investigating the Yunnan regional precipitation variation characteristics, especially the wet season trends, is of vital scientific significance and can provide reliable information that could be used to improve disaster prevention and mitigation.

2 Data and methods

This paper uses observation data collected from 124 stations (Fig. 1(a)) over Yunnan Province, the monthly wind re-analysis data (2.5° × 2.5°) from National Centers for Environmental Prediction (NCEP, USA)/National Center for Atmospheric Research (NCAR, USA) (Kalnay et al., 1996), and the monthly sea surface temperature (SST) data (1° × 1°) from the Meteorological Office, Hadley Centre, UK (Rayner et al., 2003). The data covered the period of 1961–2011. The CMIP5 monthly data used for wind projection were derived from the simulated results of seven globally coupled ocean–atmosphere models from the Intergovernmental Panel on Climate Change 5th Assessment Report (IPCC AR5). This included the 1961–2005 data from a historical simulation experiment and the 2006–2020 data predictions by the RCP4.5 experiment for future scenario projections, which represents the moderate emission of greenhouse gases (GHG). The basic information from the seven models is shown in Table 1. See http://pcmdi-cmip.llnl.gov/cmip5/availability.html for more detailed information.

The statistical methods adopted in this paper were correlation analysis, moving average treatment, the use of least squares to calculate linear trends, and composite analysis. To compare the wind reanalysis data, the bilinear interpolation method (Wang et al., 2006) was used to re-grid the above-mentioned model results to 2.5° × 2.5° grids (Wild and Schmucki, 2011; Polade et al., 2013).

Table 1 Climate model details

No.	Model	Research institute	Resolution (meridional × zonal)
1	bcc-csm1-1	Beijing Climate Center, China Meteorological Administration	2.8° × 2.8°
2	CCSM4	National Center for Atmospheric Research	1.25° × 0.94°
3	FGOALS-g2	LASG, Institute of Atmospheric Physics, Chinese Academy of Sciences; and CESS, Tsinghua University	2.8° × 2.8°
4	FGOALS-s2	LASG, Institute of Atmospheric Physics, Chinese Academy of Sciences	2.8° × 1.66°
5	GFDL-CM3	Geophysical Fluid Dynamics Laboratory	2.5° × 2.0°
6	HadGEM2-AO	National Institute of Meteorological Research/Korea Meteorological Administration	1.875° × 1.25°
7	MPI-ESM-LR	Max Planck Institute for Meteorology (MPI-M)	1.875° × 1.87°

Previous studies noted that the root mean square error of the ensemble means of the models was lower than that for the individual models (Lambert and Boer, 2001), indicating that more reliable predictions can be acquired using ensembles (Tebaldi and Knutti, 2007). Therefore, an equivalent weighted average (arithmetic mean value) was calculated for the seven models.

3 Variation characteristics for precipitation across the Yunnan region

Significant differences in precipitation across the Yunnan region are evident between the dry and wet seasons. Figure 1 shows the annual precipitation cycle for 124 meteorological stations located across the Yunnan region between 1961 and 2011. Figure 1(b) suggests that the monthly rainfall has a unimodal pattern. The southwest monsoon means that the wet season begins in May and lasts until October. During this period, there is a high amount of rainfall in June, July and August, with the monthly mean precipitation exceeding 180 mm. The dry season extends from November to the next April, with monthly rainfall less than 50 mm. The precipitation data show that spring, summer, autumn, and winter (Fig. 1(c)) account for 16.3%, 55.2%, 23.9%, and 4.6% of annual precipitation, respectively. The accumulated rainfall for summer and autumn accounts for more than 75% of the annual total, so any changes in those precipitation levels will have a major impact on potential flood and drought events over this region. This study defines summer (JJA) and autumn (SON) as the wet season and will analyze the rainfall characteristics for this period.

Figure 2 shows annual and wet season precipitation variations in Yunnan over the past 50 years. The seasonal precipitation shows significant interannual and interdecadal variations. Generally speaking, annual, summer, and autumn seasonal, precipitation levels have decreased by varying degrees, yet increased in spring and winter (data not shown). The annual precipitation linear trend was 153.5 mm/100 yr, for summer it was 170.4 mm/100 yr, and for autumn it was 62.5 mm/100 yr. The summer precipitation trend was significant at the 95% level. The curves obtained by using the moving average method showed that summer precipitation (Fig. 2(c)) was abnormally high from the 1960s to the early 1970s, but then fell below average until the early 1990s. Another pluvial or wet period began in 1993, but after 2003, the area again experienced periods of minimal rainfall. In the 1980s, there was a decrease in interdecadal variation characteristics for autumn precipita-

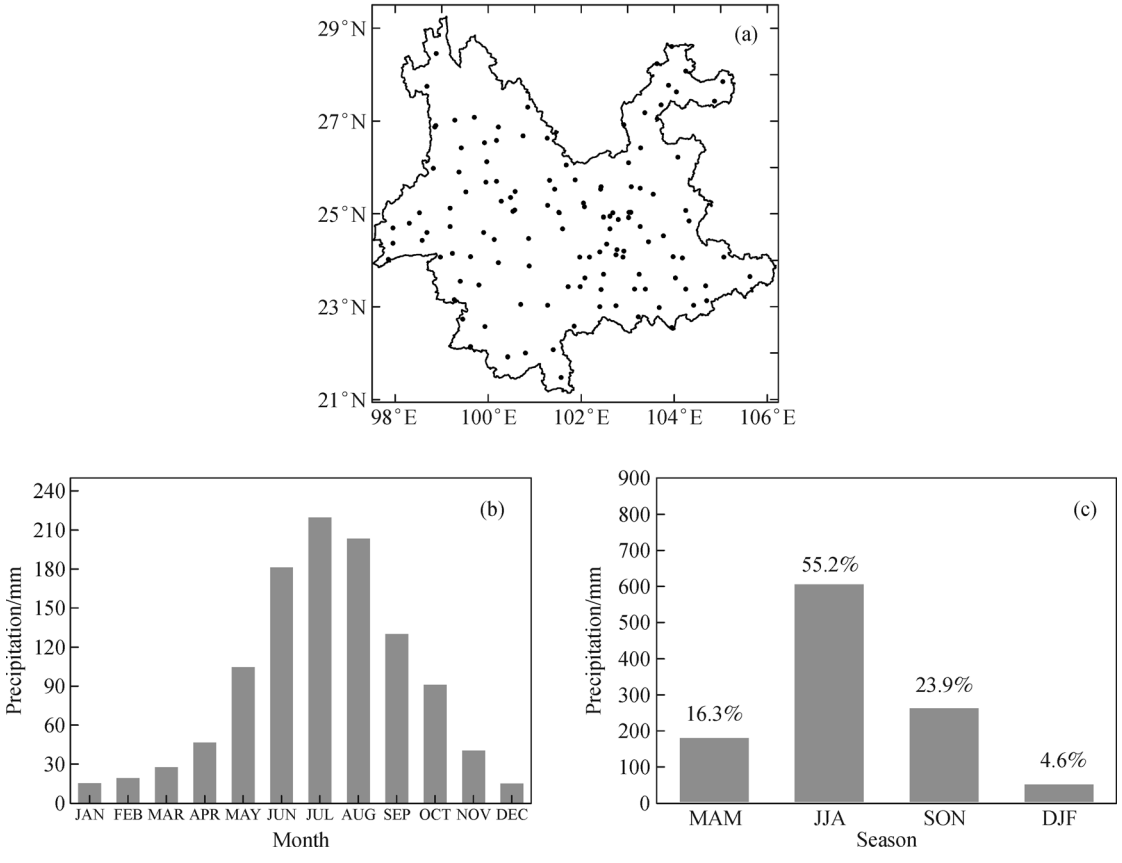

Fig. 1 Locations of 124 meteorological stations in Yunnan Province (a); annual precipitation cycle data from 124 meteorological stations in Yunnan Province between 1961 and 2011 (b, c; unit: mm).

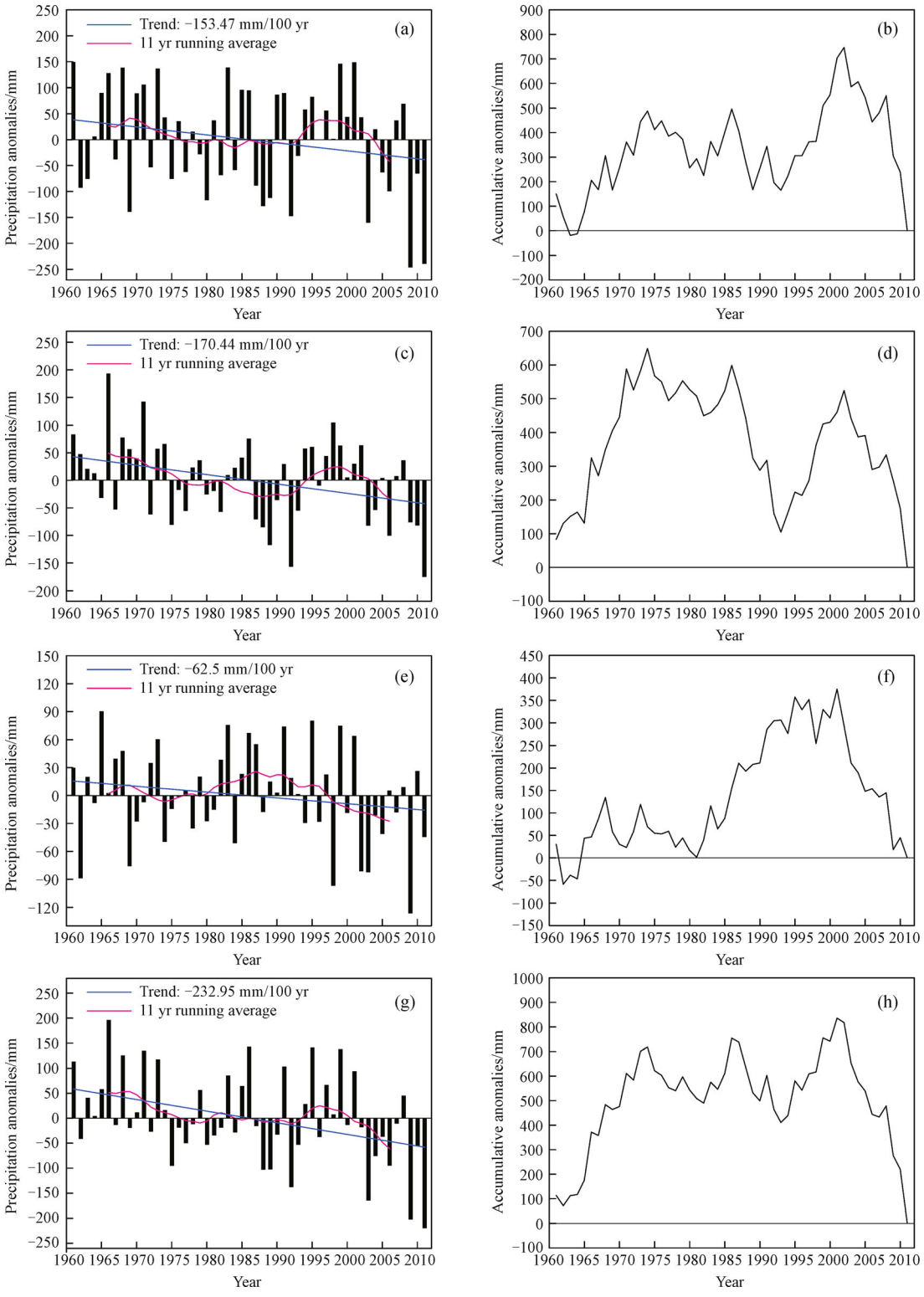

Fig. 2 Time series for precipitation (a, c, e, g, red lines represent 11 yr running average, blue lines are the linear trends, unit: mm) and cumulative anomaly curves between 1961 and 2011 (b, d, f, h, unit: mm); (a, b) annual, (c, d) JJA, (e, f) SON, (g, h) JJA and SON accumulations.

tion (Fig. 2(e)). Precipitation increased from the early 1980s to 2000, but subsequently decreased showing a negative anomaly in both summer and autumn. We analyzed the precipitation over the two seasons and obtained a time series for precipitation variation in the wet season (summer and autumn) (Fig. 2(g)). The summer (JJA) and autumn (SON) precipitation linear trend was 233.0 mm/100 yr, which was significant at the 95% level. When compared with the annual precipitation (Fig. 2(a)), we can see similar interdecadal variation patterns in that both show a continual decreasing trend after the early 2000s. These results indicate a reduction in precipitation over the Yunnan region in recent years and that the occurrence of successive drought disasters has primarily been caused by the negative precipitation anomaly in the wet season.

Figures 2(b)–2(h) show the yearly variation curves for precipitation anomaly accumulation, clearly indicating precipitation changes over the different seasons. There are many phases of interdecadal oscillation and the turning points on the curves show when wet periods and dry periods appeared. The cumulative anomaly series for JJA precipitation shows a double-peaked shape over the past 50 years (Fig. 2(d)), and every peak pattern corresponds to one variation cycle of the decadal positive and negative precipitation phases. In this cumulative anomaly curve, 1993 to 2002 was a wet period and 2002 to 2011 was a dry period. The SON cumulative precipitation anomaly has a single-peak pattern after 1980 (Fig. 2(f)), different from the JJA precipitation, and has a longer variation cycle. From 1980 to 1995, precipitation increased and remained stable for a short period, but in 2000, it decreased, resulting in a dry period. The annual precipitation decreased after 2000, as did the JJA and SON accumulations (Figs. 2(b) and 2 (h)). Thus, it is shown that the period since 2000, experiencing significantly less rainfall, was the negatively contributing factor for the cumulative precipitation anomaly over the past 50 years in Yunnan. However, the principal cause was the decrease in JJA and SON.

In summary, the JJA and SON precipitation accounts for a large proportion of the annual precipitation, but the JJA and SON cycle variations are different. The JJA and SON precipitation phases overlap after 2000, especially during the dry periods where they significantly influence the drought event frequency over Yunnan. It is important to understand the circulation background behind such changes in precipitation for the two seasons so that we can predict future trends.

4 Analysis of the circulation background behind the precipitation anomalies

Precipitation anomalies are usually related to changes in atmospheric circulation over a given period of time. We analyzed the statistical relationships between precipitation and circulation anomalies in summer (JJA) and autumn (SON) by investigating the atmospheric circulation backgrounds. We chose a significantly abnormal dry year and wet year by standardizing the precipitation series for JJA and SON (Fig. 3). The years with standardized anomaly values >1 are wet years while the years with standardized anomaly values < -1 are dry years. We selected periods with approximate anomaly values of >0 as wet periods, and values of <0 as dry periods (Table 2).

4.1 Analysis of the summer circulation field

The correlation between precipitation and wind fields over Yunnan was investigated. Figures 4(a) and 4(b) show the correlation analyses between summer precipitation and the 700 hPa and 200 hPa wind fields. The shaded areas show where the results were significant at the 95% or 99% confidence levels. It was observed that from west to east

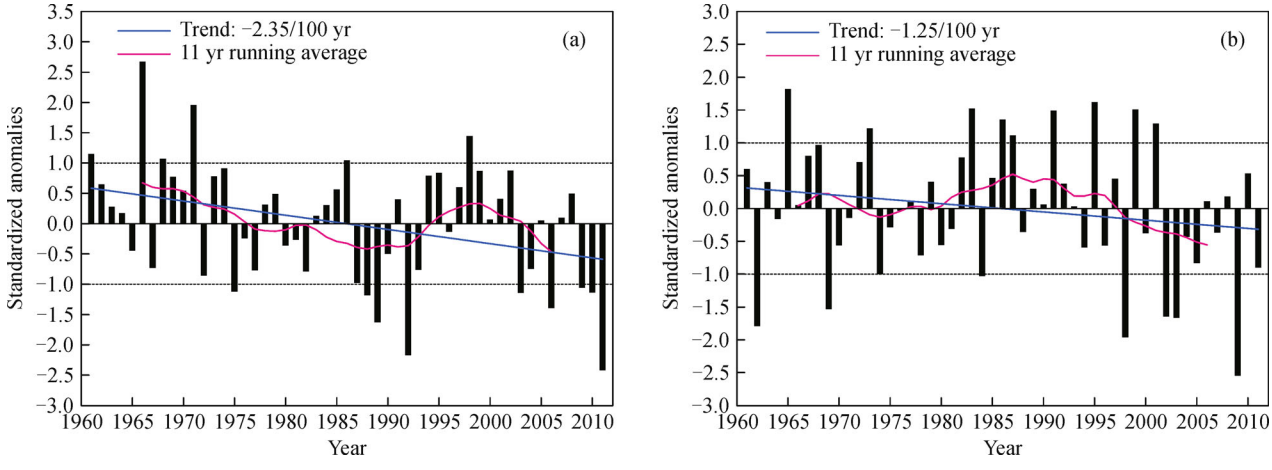

Fig. 3 Time series for (a) JJA and (b) SON standardized precipitation between 1961 and 2011 (dashed line is the boundary of ±1 standardized anomalies, red line represents 11 yr running average, blue line is the linear trend, unit: 1).

Table 2 The wet and dry years (periods) for JJA and SON

	Summer (JJA)	Autumn (SON)
Wet year	1961, 1966, 1968, 1971, 1986, 1998	1965, 1973, 1983, 1986, 1987, 1991, 1995, 1999, 2001
Dry year	1975, 1988, 1989, 1992, 2003, 2006, 2009, 2010, 2011	1962, 1969, 1984, 1998, 2002, 2003, 2009
Wet period	1961–1971, 1994–2002	1986–2001
Dry period	1987–1993, 2003–2011	2002–2011

— over the southern Arabian Peninsula, the tropical Indian Ocean, the Bay of Bengal, the Indo-China Peninsula, and the area between the Peninsula and the Philippines — the 700 hPa wind had a high correlation with the Yunnan summer precipitation. This suggested that the moisture for the Yunnan summer precipitation came not only from the Bay of Bengal, brought on by the southwest winds, but also from the Western Pacific warm pool carried by the southeast winds. In addition, it is noteworthy that the summer precipitation over Yunnan was positively correlated with the abnormal southerly wind over the East Asian monsoon region, the abnormal cross-equatorial flows from the Southern Hemisphere over the East Indian Ocean and 130°E, and with the abnormal westerly wind from the Bay of Bengal to the Indo-China Peninsula.

In the 200 hPa high-level wind field, the Chinese mainland was mainly dominated by abnormal cyclones whereas the western Tibetan Plateau was controlled by abnormal anticyclones. Between the two abnormal systems, significant north winds blew over the Tibetan Plateau at 200 hPa, while the tropical Indian Ocean experienced significant easterly winds. When the South Asia High position leans towards the west and the Western Pacific Subtropical High is weak, Yunnan tends to have more rain in summer, while at the same time, the tropical vertical circulation over the Indian Ocean is abnormally strong. Monsoon activity, the South Asian High, and the Western Pacific Subtropical High significantly affect the East Asian summer climate. The analysis shows that the cross-equatorial flows of the low-level Indian Ocean and the Western Pacific, the winds from the Bay of Bengal to the Indo-China Peninsula, and the South Asia High over the Tibetan Plateau are the critical weather systems that influence summer precipitation in Yunnan.

We used the summer wet and dry years' data (Table 2) to analyze the composite mean difference field for the high-level and low-level winds in the troposphere for both annual and interdecadal variation during corresponding periods. Figures 5(a) and 5(b) show the composite difference field between the low-level and high-level wind fields for the JJA wet and dry years. The shaded areas show where the results were significant. The 700 hPa low-level wind field data show that, during wet years, anomalous southerly winds consistently appear over eastern China, abnormal southwest winds blow from the Bay of Bengal to the Indo-China Peninsula, and stronger cross-equatorial flows are observed from the Southern Hemisphere over the Eastern Indian Ocean and 130°E (Fig. 5(a)). Notably, abnormal westerly winds appear over Yunnan and the northern Indo-China Peninsula, and the vapor transport from the Bay of Bengal is stronger. The difference in the wind field at the 200 hPa level between wet and dry years is shown in Fig. 5(b). The eastern Tibetan Plateau is dominated by anomalous cyclones, while the western plateau is under the control of anomalous anticyclones. The 200 hPa wind field over the Tibetan Plateau is dominated by significantly abnormal northerly

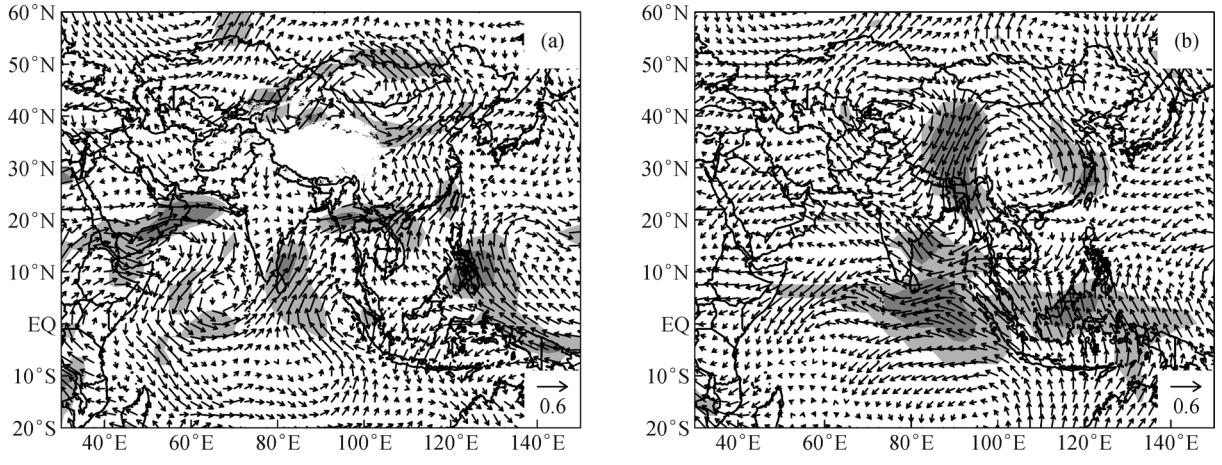

Fig. 4 Correlation vectors between summer precipitation and the wind vector distribution at (a) 700 hPa and (b) 200 hPa. The correlation vectors are structured by the correlation coefficient between precipitation and meridional wind for the *X* direction and the zonal wind for the *Y* direction. The light and dark shaded areas are significant at 95% and 99%, respectively, unit: 1.

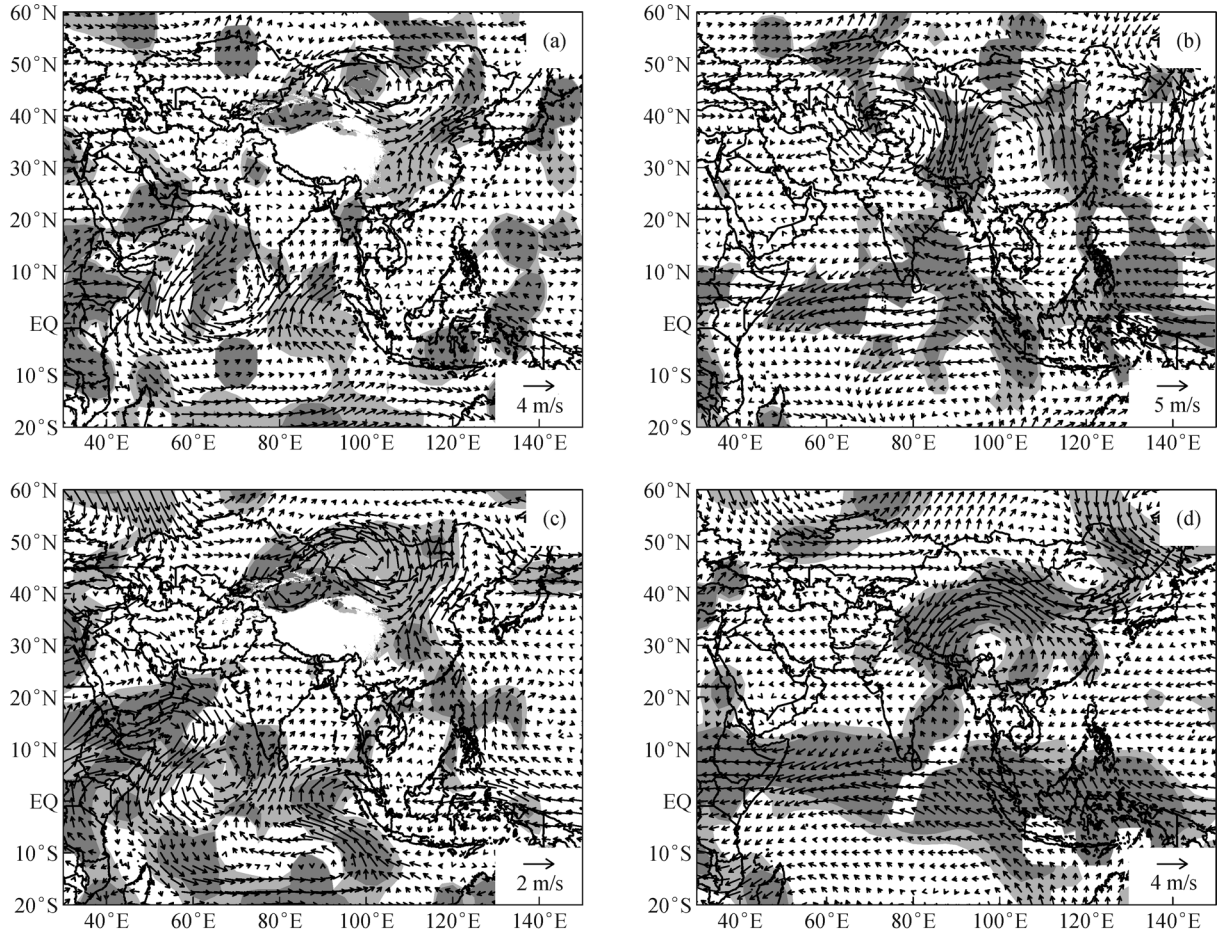

Fig. 5 Wind difference maps for JJA wet and dry years (a, b, wet years minus dry years), wet and dry periods (c, d, wet periods minus dry periods). The *F*-test was used to compare the (a, c) 700 hPa, (b, d) 200 hPa wind fields (unit: m/s, the light and dark shaded areas show that the results were significant at 95% and 99%, respectively).

winds, whereas the tropical Indian Ocean is controlled by anomalous easterly winds. The 200 hPa dipole pattern for anomalous circulations over the east and the west of the Tibetan Plateau are most likely related to zonal oscillations at the center of the South Asia High. Some studies suggest that when the location of the South Asia High center leans toward the east, precipitation amounts typically decrease in southern China, including Yunnan (Wei et al., 2013). When the South Asia High moves northwards, it simultaneously extends to the east, thus promoting the formation of a circulation condition that leads to a decrease in summer precipitation over southwest China. Movement of the South Asia High to the north is negatively correlated to precipitation in southwest China (Lu et al., 1987; Li et al., 2012).

Periods with either greater or less than average summer precipitation are shown in Table 2. The interdecadal variation in the composite difference field data was investigated (Figs. 5(c) and 5(d)). These figures show that the distribution of the 700 hPa anomalous wind field difference values in summer wet and dry periods were very similar to the composite wind field (Fig. 5(a)) for the interannual variation, except that the notable southerly wind over the mainland was primarily from the South China Sea and the western Pacific Ocean. In comparison with Fig. 5(a), the strong westerly wind from the Bay of Bengal to the Indo-China Peninsula has disappeared, which possibly suggests that the interannual variation for summer precipitation over Yunnan is closely related to moisture transportation from the Bay of Bengal, while the interdecadal variation is associated with vapor transport from the South China Sea and the Pacific Ocean. The 200 hPa wind difference field results were similar to the analysis results for typical wet and dry years. However, the abnormal anticyclone activity over the western Tibetan Plateau was not obvious, which indicated that the Western Pacific Subtropical High anomaly had a greater effect on the interdecadal differences than did the other highs.

4.2 Autumn circulation analysis

We also analyzed the atmospheric circulation field in autumn. Figure 6 shows the correlations between the autumn precipitation over Yunnan and the wind field

indicating that the autumn precipitation over Yunnan was poorly correlated with the 700 hPa wind field (Fig. 6(a)). This may be due to the seasonal reversal from summer to winter during autumn, which destabilizes the circulation pattern. However, it is still possible to see the marked correlation zones. These include west Asia, the Bay of Bengal, the mid-latitude zones over East Asia, and the Western Pacific warm pool area. In relation to the summer occurrences (Fig. 4(a)), to those in autumn over the Bay of Bengal, the southeast airflow blows from the South China Sea, and the southerly winds over the eastern section retreat onto the sea. In the high-level wind field at 200 hPa (Fig. 6(b)), the area to the east of the Tibetan Plateau was controlled by an anomalous anticyclone while the Plateau was dominated by significantly abnormal southerly winds. This suggests that in the pluvial years over Yunnan, the South Asia High withdraws from the plateau later, and the Western Pacific Subtropical High is stronger and leans towards the west. As compared with the situation in summer (Fig. 4(b)), the significant anomalous easterly winds in the tropics typically blew over the east Indian Ocean and the oceanic continent, and the mid-latitude west Asia region had a notable anomalous cyclone with marked abnormal northerly winds near 60°E.

The composite difference field was analyzed using the chosen autumn wet and dry years. The wet and dry period data are shown in Table 2. The results showed that in wet years, eastern China, and especially the North and Northeast China regions, experienced extremely abnormal northerly winds in the low-level wind field at 700 hPa (Fig. 5(a)). Furthermore, anomalous southerly winds blew over the area from the Bay of Bengal to Indo-China to the Peninsula. This phenomenon indicates that, in years with more autumn rains, the autumn cold air activities over North China became stronger and the warm humid air flows from the Bay of Bengal increased, creating cold and warm air fronts over Yunnan, which resulted in increased precipitation. Moreover, the most notable feature in the upper-air difference field at 200 hPa was a strong abnormal anticyclone over the mid-latitude area of west Asia.

Figures 7(c) and 7(d) show the composite wind field differences for wet and dry periods at 700 hPa and 200 hPa. At 700 hPa, the abnormal wind distributions are similar to the composite wind field distribution (Fig. 7(a)) for interannual variation, although the cross-equatorial airflows over the central Indian Ocean and the southerly airflows over the Bay of Bengal are relatively stronger. At 200 hPa, a disturbed wave-like pattern, which indicates an "anticyclone–cyclone–anticyclone" anomalous circulation, formed along the line over the "Middle East–Tibetan Plateau–East Asia" area at around 25°N (Fig. 7(d)). The wave patterns at the circumglobal scale have been studied by a number of scientists (Watanabe, 2004; Ding and Wang, 2005, 2007; Huang et al., 2011; Huang et al., 2013). Yang et al. (2012) obtained a similar wave pattern when analyzing the winter precipitation anomaly over Yunnan Province. This type of wave structure may reflect the influence of the Asian subtropical westerly jet on the southern branch trough over the Bay of Bengal. When the jet stream strengthens, quasi-stationary wave energy spreads from the Middle East to East Asia and prompts the deepening of the Tibetan Plateau–Bay of Bengal trough (Ji et al., 2008), which contributes to the formation of precipitation over Yunnan. This wave-like anomaly pattern is shown in Fig. 7(b) and Fig. 6(b), which have consistent distribution patterns, but with slightly different intensities and locations. Our analysis has identified the anomalous distribution features of the typical circulations that affect autumn precipitation over Yunnan.

5 Analysis of sea temperature anomalies

Many studies have shown that the sea surface temperature

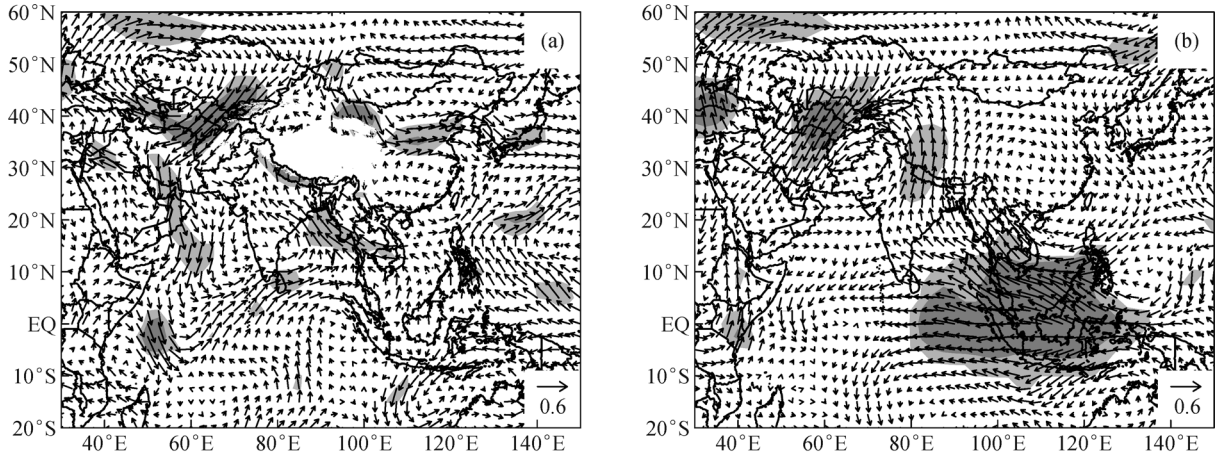

Fig. 6 Correlation vectors between autumn precipitation and the wind vector distribution at (a) 700 hPa, (b) 200 hPa. The correlation vectors are structured by the correlation coefficient between precipitation and meridional wind for the *X* direction and the zonal wind for the *Y* direction. The light and dark shaded areas show that the results were significant at 95% and 99%, respectively, unit: 1.

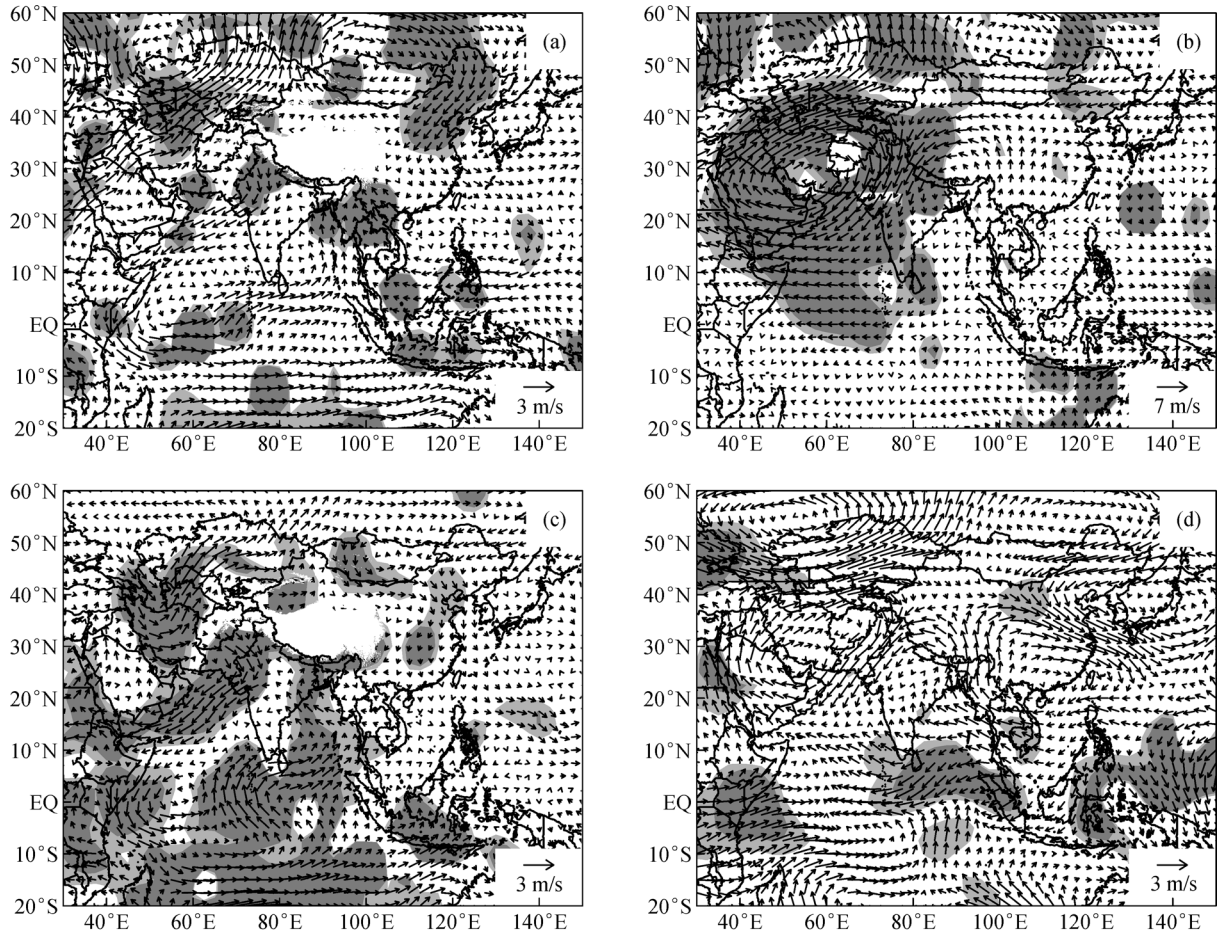

Fig. 7 Autumn wind difference maps for JJA wet and dry years (a, b, wet years minus dry years), wet and dry periods (c, d , wet periods minus dry periods). The *F*-test was used for the (a, c) 700 hPa, (b, d) 200 hPa wind field data (unit: m/s, the light and dark shaded areas show where the results were significant at 95% and 99%, respectively).

(SST), especially the SST anomalies in the Pacific (Chang et al., 2000; Wang et al., 2000; Jin and Chen, 2002) and Indian Oceans (Xiao et al., 2002; Yang et al., 2007; Li et al., 2010), affect the Asian monsoons and thus cause significant changes to the East Asia climate. Figure 8(a) shows the correlation coefficient distribution between the summer precipitation series over Yunnan and SST over the same period. The entire Indian Ocean basin has a consistent negative correlation while parts of the northern Pacific Ocean have a significant positive correlation. The Indian Ocean warm pool SST near the equator is negatively correlated to summer precipitation. In summer, land warms up quickly, but the ocean warms up slowly due to the large oceanic thermal inertia. These ocean–land thermal contrasts critically affect Asian monsoons. The negative SST anomaly in the Indian Ocean increases the north–south thermal contrast between land and ocean resulting in both an increased intensity in the South Asian monsoon and in the moisture conveyed to Yunnan and other regions of China by the southwest airflow from the Bay of Bengal. As seen in Fig. 5(a), abnormal southwest winds blow over the southern Indian Ocean and from the Bay of Bengal to the Indo-China Peninsula when the wind field is 700 hPa. Figure 5(b) shows that in the 200 hPa wind field, the tropical Indian Ocean is controlled by anomalous easterly winds. These conditions promote precipitation in summer over Yunnan. Zhang (2012) studied heat and vapor transport and found that the positive anomaly produced by the warm pool surface latent heat flux over the Indian Ocean in August caused the monsoon circulation to weaken, which reduced precipitation over the low-latitude plateau region.

The patterns of the correlation coefficient distributions for autumn precipitation and SST differ from those for summer (Fig. 8(b)). The autumn precipitation over Yunnan was negatively correlated to the SST from the tropical western Pacific Ocean to the eastern Indian Ocean. Meanwhile, an area with significant positive correlation appeared in the northeast Pacific Ocean around 20°N. The study of Jin and Chen (2002) indicated that when the warm anomaly occurs in the Western Pacific warm pool, the meridional winds over the Bay of Bengal, the Indo-China

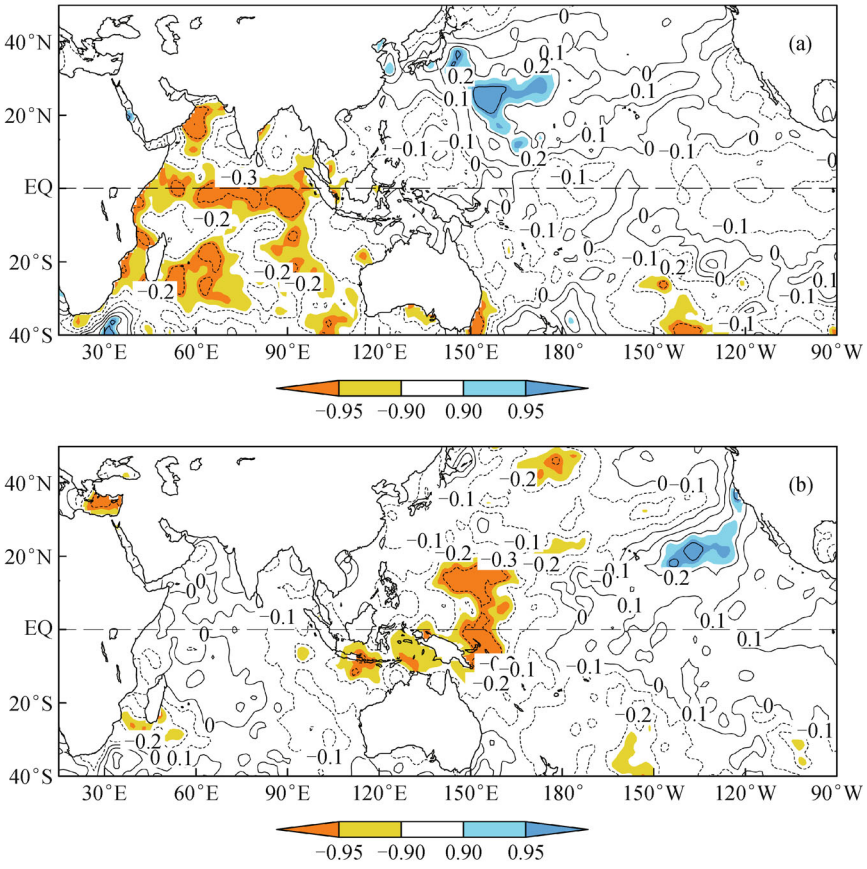

Fig. 8 Precipitation series and corresponding sea surface temperature correlation coefficients in (a) summer and (b) autumn (unit: 1; shaded areas show results that are significant at>90%, based on the *t*-test.)

Peninsula, and the South China Sea, etc. have characteristics that weaken the summer monsoon over the equatorial eastern Indian Ocean and the western Pacific Ocean. Autumn is the season when Asian summer monsoons gradually fade and finally retreat. On the basis of the above causes, when the autumn warm anomaly appears over the Western Pacific warm pool, the intensity of the summer monsoon is weaker or the summer monsoon retreats earlier. By combining the above discussion on winds, we can see that the Indian Ocean SST has considerable influence on summer precipitation over Yunnan, while the Pacific Ocean SST has a greater influence on autumn precipitation.

6 Circulation field simulation and projection by CMIP5

The models shown in Table 1 have improved Asian monsoon simulations. Some models reproduce better moisture transport patterns over the Asian–Australian monsoon region than others, including bcc-csm1-1, CCSM4, FGOALS-s2, and MPI-ESM-LR (Song et al., 2013). A 4–6 year period in the Tibetan high was simulated by FGOALS-s2 and FGOALS-g2. The simulated Tibetan Plateau precipitation values in FGOALS-s2 and bcc-csm1-1 seemed to be superior to the other models (Duan et al., 2013). Some previous studies (Xu and Xu, 2012; Zhou and Xiao, 2014) have suggested that future projections using CMIP5 data show that Yunnan Province and its southern areas might be relatively dry up to 2020. Because of the limited capability of the new-generation global ocean–atmosphere coupled model to simulate the climate in Yunnan and its surrounding areas, and especially the great uncertainty present when projecting precipitation directly, we decided to provide an atmospheric dynamic basis for the above conclusion by using wind data to analyze the circulation background. In Section 4, we discussed the circulation characteristics of the summer and autumn anomalous precipitations over the Yunnan region. Here, we discuss whether the circulation background causes the precipitation anomaly over Yunnan by analyzing the CMIP5 data, and will also explore the potential future precipitation trend.

6.1 Simulation of the summer circulation field

We used the simulation data on the historical atmosphere

obtained from the Historical Experiment Group for CMIP5 to assess whether the modeling results could simulate previous wet and dry periods. Figure 9(a) shows the abnormal wind distributions modeled during the summer dry period identified in Table 2. It can be seen that in the dry periods (Fig. 9(a)), there was a consistent significant easterly anomaly over the northern Indian Ocean and a northeasterly anomaly from the Bay of Bengal to the Indo-China Peninsula at 700 hPa. This suggests that in the simulated wind field during the dry period, the cross-equatorial westerly flow and the southwesterly flow over the Bay of Bengal were weaker. This result was similar to that from the previous analysis based on the observation data. In the 200 hPa simulated circulation (Fig. 9(c)), there was a southerly wind above the Tibetan Plateau, the area to the east of the plateau had an anticyclonic circulation, the area to its west was under an abnormal cyclonic circulation, and the tropical Indian Ocean region was controlled by an abnormal westerly wind. It can be easily seen that these characteristics agreed with the observational data analysis results (Section 4) for the summer dry periods over Yunnan. Therefore, the wind simulation by the model does reflect the anomalous circulation features when either more or less precipitation occurs over this region. Based on this conclusion, we investigated the wind output from 2010–2020 under the RCP4.5 modeling scenario. Figure 9(b) shows the abnormal wind field at 700 hPa during this time period. It can be seen that over the tropical Indian Ocean and the Bay of Bengal, there is an easterly anomaly that is consistent with the dry periods identified in the records. Although a westerly wind exists over eastern China, almost no southerly wind can be found, and the Indo-China Peninsula is controlled by anti-cyclones. The upper-air chart at 200 hPa (Fig. 9(d)) for the projected 2010–2020 period wind field under the RCP4.5 scenario also shows a) the significant strong westerly anomaly over the Indian Ocean, b) the area to the west of Tibetan Plateau is under the control of cyclonic circulation, and c) there are southerly wind flows above the plateau. This finding is similar to the recorded circulation patterns identified in the dry period. In summary, the projected result of the CMIP5 model under the future RCP4.5 scenario indicates that the monsoon circulations over the Indian Ocean and South China Sea in summer

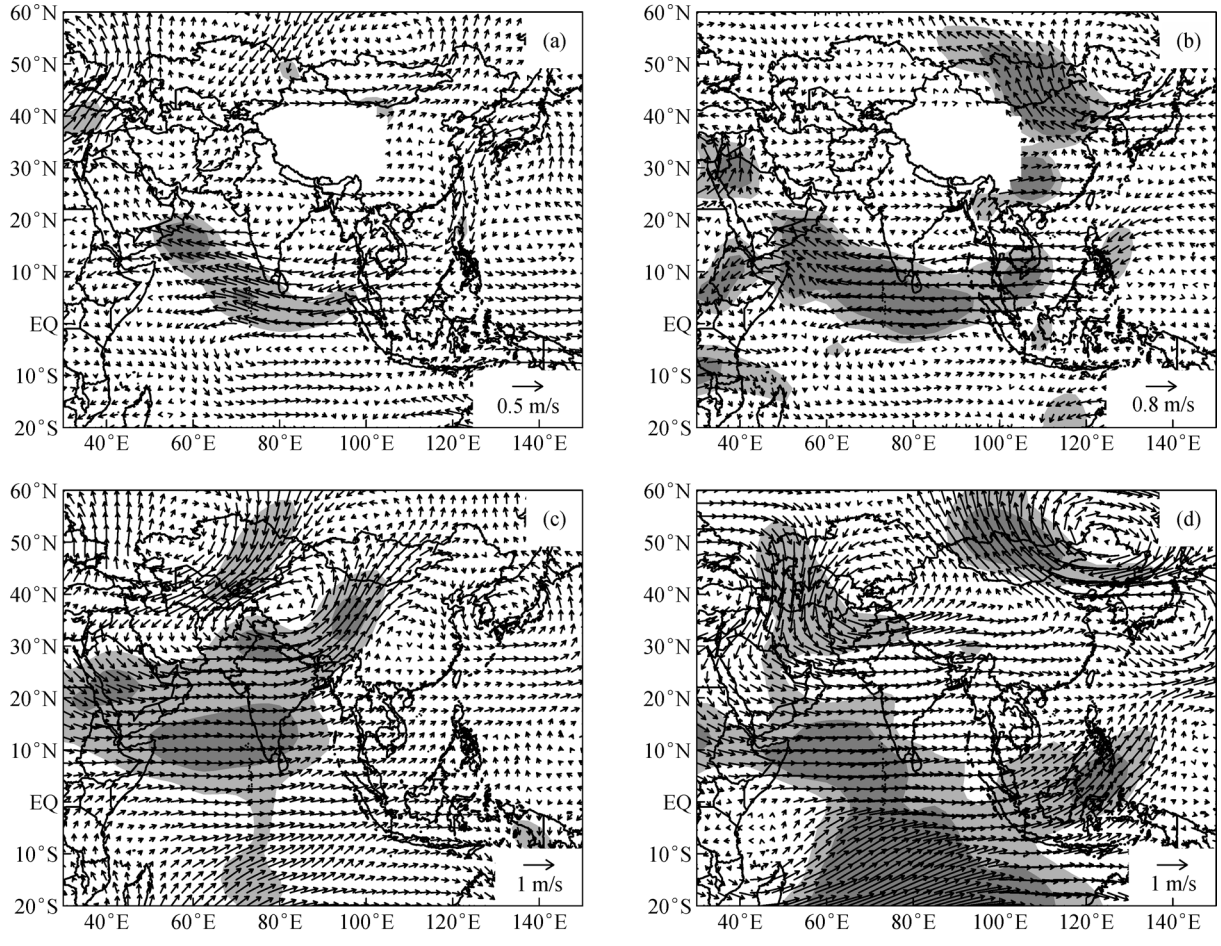

Fig. 9 Model-simulated abnormal circulation fields in dry periods during summer (a, c), and the projected abnormal circulation fields for 2010–2020 (b, d) (relative to the 1961–2011 recorded means); wind fields (a, b) at 700 hPa and (c, d) at 200 hPa (unit: m/s, the light and dark shaded areas show where results are significant at 95% and 99%, respectively).

may reduce precipitation in Yunnan between 2010 and 2020.

6.2 Simulation of the autumn circulation field

The modeled simulation result of the wind anomaly at 700 hPa for the historical dry periods in autumn show the anomalous northeast wind over southern China (Fig. 10 (a)). The eastern coast of China lies on the edge of anomalous cyclones, the South China Sea is dominated by the northwest wind, and the Indo-China Peninsula is dominated by westerly winds which reduce moisture transport from the western Pacific and the South China Sea to the Yunnan region. In the 200 hPa wind field (Fig. 10 (c)), eastern China is controlled by a cyclonic circulation, the Indo-China Peninsula is under the influence of anomalous westerly winds, and the tropical eastern Indian Ocean and equatorial regions of the oceanic continent are under the control of light westerly winds. Although the intensity and location are not particularly accurate, the general situation basically agrees with the abnormal wind characteristics of the autumn dry periods over Yunnan obtained by observational data analysis. Similarly, we analyzed the model-simulated results of the 2010–2020 abnormal winds under the RCP4.5 scenario. Figure 10(b) shows the abnormal wind features at 700 hPa. It can be seen that the Chinese mainland has anomalous northerly winds and the Indo-China Peninsula has anomalous northwesterly winds. The 200 hPa wind field data shown in Fig. 10(d) indicate that eastern China is under the control of a cyclonic circulation, the Tibetan Plateau has significant abnormal westerly winds, and the tropical eastern Indian Ocean and the equatorial regions of the oceanic continent are dominated by westerly winds. Along the line representing the "Middle East–Tibetan Plateau–East Asia" area, there is one anomalous wave-like pattern of "cyclone–anticyclone–cyclone," which is similar to the circulation pattern shown in Fig. 7(d). Therefore, between 2010 and 2020, it is possible to see the typical characteristics of wind circulation anomalies that coincide with the dry period over the Yunnan region, and also that autumn precipitation over the region may decrease.

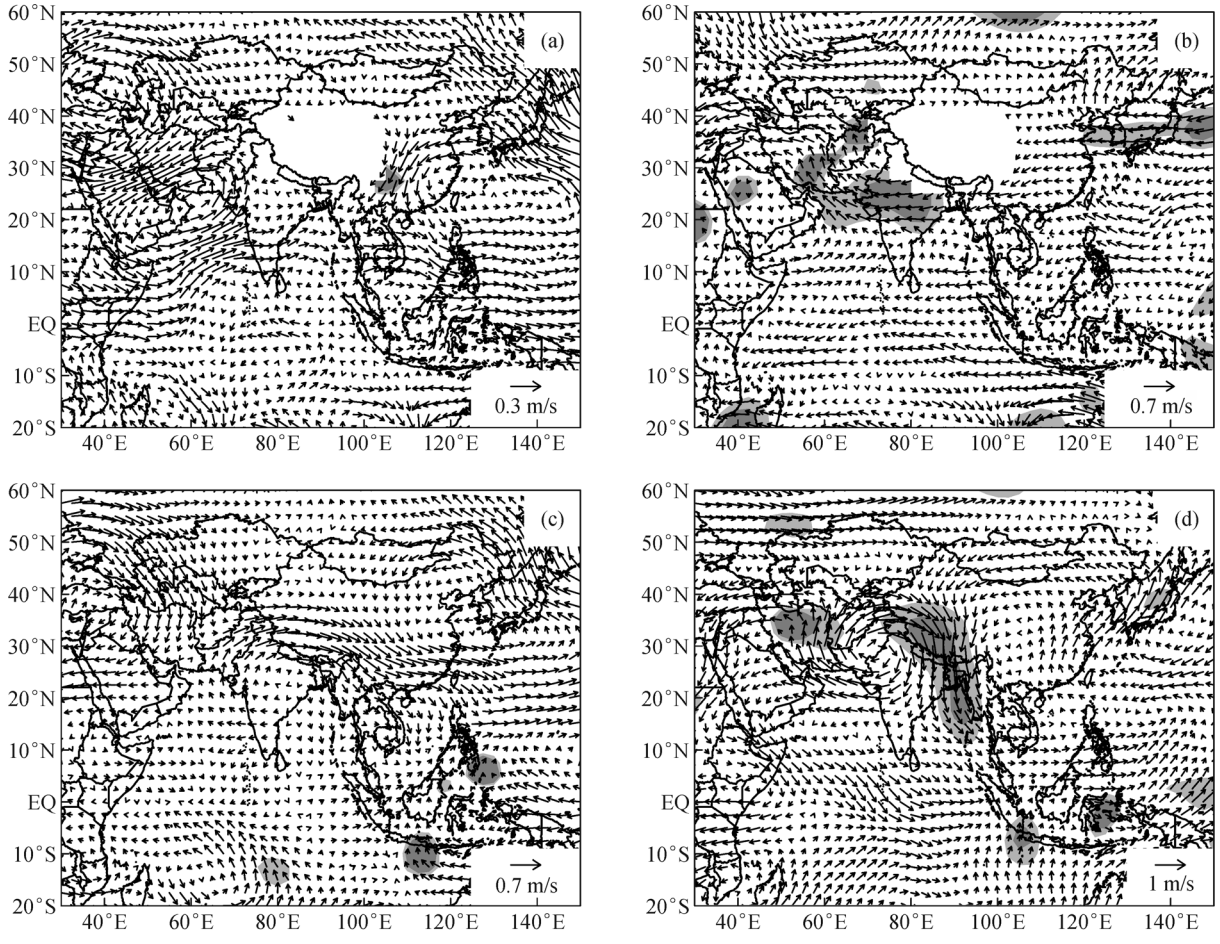

Fig. 10 Model-simulated abnormal circulation fields in dry periods during autumn (a, c) and the projected abnormal circulation fields for 2010–2020 (b, d) (relative to the 1961–2011 recorded means); (a, b) at 700 hPa and (c, d) at 200 hPa (unit: m/s, the light and dark shaded areas are where results were significant at 95% and 99%).

7 Conclusions

In this study, we analyzed the basic precipitation change characteristics for Yunnan. We undertook composite analyses of the high- and low-level circulation fields in the troposphere in order to study the interannual and interdecadal variations. We investigated the circulation backgrounds in the wet and dry periods during summer and autumn, their correlations to SST, and predicted the circulation anomalies for the 2010–2020 time period based on the CMIP5 data. The main conclusions of the research are as follows:

1) The precipitation across Yunnan shows distinct differences between the dry and wet seasons. The cumulative precipitation in summer and autumn accounts for more than 75% of the annual total precipitation, which means that summer and autumn represent the wet season in this region. The linear trend for summer and autumn cumulative precipitation over the past 50 years was 233.0 mm/100 yr. Both the summer and autumn precipitation data have remarkable interdecadal oscillation features, but the cycle characteristics of the two are not completely similar. Since 2000, precipitation during summer and autumn has decreased resulting in a dry period. This overlap in dry phases has significantly contributed to the successive drought events across Yunnan in recent years.

2) The atmospheric circulation characteristics that correspond to the high or low precipitation periods over Yunnan in summer and autumn are notably different. The data suggests that anomalous circulation backgrounds at the temporal interannual variation and interdecadal variation scales were very similar and significantly affected precipitation. At 700 hPa, eastern China experienced abnormal southerly winds during the summer rainy period. Remarkable abnormal southwesterly winds blew from the Bay of Bengal to the Indo-China Peninsula, and the central Indian Ocean experienced abnormal cross-equatorial airflows that entered the Northern Hemisphere. In the autumn rainy period, eastern China experienced abnormal northerly winds, and the Bay of Bengal to Indo-China Peninsula area still had relatively strong southerly airflows, but the zonal wind turned eastward. During the summer rainy period, abnormal northerly winds blew in the 200 hPa wind fields above the Tibetan Plateau, and the area to its east (i.e., above China) had a distinct cyclonic abnormal circulation, while the area to its west was under the control of an anticyclonic circulation. Such circulation patterns indicate that the South Asia High leans towards the west and that the Western Pacific Subtropical High is weak. In contrast, during the autumn dry period, the Tibetan Plateau was controlled by significant abnormal southerly winds, the area to its east was affected by an anticyclonic circulation, and the area to its west was under an abnormal cyclonic circulation. At middle latitudes from Middle East to East Asia, there was one abnormal circulation disturbance wave-like structure called a "cyclone–anticyclone–cyclone."

3) These results showed that summer precipitation over the Yunnan region was closely related to the SST anomaly in the Indian Ocean, while autumn precipitation was more closely related to the SST anomaly in the western Pacific Ocean. The amount of autumn precipitation was highly correlated with vapor transport from the South China Sea and the western Pacific Ocean.

4) The global coupled ocean–atmosphere models were quite successful at simulating the typical characteristics of the high- and low-level winds that influence the summer and autumn rainfalls over the Yunnan region. The future RCP4.5 scenario projection analysis by CMIP5 suggests that the typical features of the high- and low-level winds between 2010 and 2020 will lead to a decrease in precipitation in summer and autumn, which will likely lead to an increase in drought events over this region.

Acknowledgements This research was supported by the National Natural Science Foundation of China (Grant Nos. 41175051 and 41101045), and the National Science Foundation of China–Yunnan Province Joint Grant (U1133603).

References

Boo K O, Kwon W T, Baek H J (2006). Change of extreme events of temperature and precipitation over Korea using regional projection of future climate change. Geophys Res Lett, 33(1): 313–324

Chang C P, Zhang Y, Li T (2000). Interannual and interdecadal variations of the East Asian summer monsoon and tropical Pacific SSTs. Part I: roles of the subtropical ridge. J Clim, 13(24): 4310–4325

Chen H P (2012). Projected change in extreme rainfall events in China by the end of the 21st century using CMIP5 models. Chin Sci Bull, doi: 10.1007/s11434-012-5612-2

Deng H, Luo Y, Yao Y, Liu C (2013). Spring and summer precipitation changes from 1880 to 2011 and the future projections from CMIP5 models in the Yangtze River Basin, China. Quat Int, 304: 95–106

Diffenbaugh N S, Giorgi F (2012). Climate change hotspots in the CMIP5 global climate model ensemble. Clim Change, 114(3–4): 813–822

Ding Q, Wang B (2005). Circumglobal teleconnection in the Northern Hemisphere summer. J Clim, 18(17): 3483–3505

Ding Q, Wang B (2007). Intraseasonal teleconnection between the summer Eurasian wave train and the Indian monsoon. J Clim, 20(15): 3751–3767

Ding Y H, Sun Y, Liu Y Y, Si D, Wang Z Y, Zhu Y X, Liu Y J, Song Y F, Zhang J (2013). Interdecadal and interannual variabilities of the Asian summer monsoon and its projection of future change. Chinese Journal of Atmospheric Sciences, 37(2): 253–280 (in Chinese)

Duan A, Hu J, Xiao Z (2013). The Tibetan Plateau summer monsoon in the CMIP5 simulations. J Clim, 26(19): 7747–7766

Frich P, Alexander L, Della-Marta P, Gleason B, Haylock M, Klein Tank A M G, Peterson T C (2002). Observed coherent changes in climatic

extremes during the second half of the 20th century. Climate Res. 19: 193–212

García-Herrera R, Paredes D, Trigo R M, Trigo I F, Barriopedro D, Hernández E, Mendes M A (2007). The outstanding 2004/05 drought in the Iberian Peninsula: associated atmospheric circulation. J Hydrometeorol, 8(3): 483–498

Huang G, Liu Y, Huang R (2011). The interannual variability of summer rainfall in the arid and semiarid regions of Northern China and its association with the northern hemisphere circumglobal teleconnection. Adv Atmos Sci, 28(2): 257–268

Huang R H, Liu Y, Feng T (2013). Interdecadal change of summer precipitation over Eastern China around the late-1990s and associated circulation anomalies, internal dynamical causes. Chin Sci Bull, 58(12): 1339–1349

Huang R H, Liu Y, Wang L, Wang L (2012). Analyses of the causes of severe drought occurring in Southwest China from the fall of 2009 to the spring of 2010. Chinese Journal of Atmospheric Sciences, 36(3): 443–457 (in Chinese)

Ji L R, Cholaw B, Shi N, Xie Z W (2008). On the medium-range process of the rainy, snowy and cold weather of South China in early 2008 Part III: pressure trough over the Tibetan Plateau/Bay of Bengal. Climatic and Environment Research, 13(4): 446–458 (in Chinese)

Jin Z H, Chen J (2002). A composite study of the Influence of SST warm anomalies over the western Pacific warm pool on Asian summer monsoon. Chinese Journal of Atmospheric Sciences, 26(1): 57–68 (in Chinese)

Kalnay E, Kanamitsu M, Kistler R, Collins W, Deaven D, Gandin L, Iredell M, Saha S, White G, Woollen J, Zhu Y, Leetmaa A, Reynolds R, Chelliah M, Ebisuzaki W, Higgins W, Janowiak J, Mo K C, Ropelewski C, Wang J, Jenne R, Joseph D (1996). The NCEP/NCAR 40-year reanalysis project. Bull Am Meteorol Soc, 77(3): 437–472

Korecha D, Barnston A G (2007). Predictability of June–September rainfall in Ethiopia. Mon Weather Rev, 135(2): 628–650

Lambert S J, Boer G J (2001). CMIP1 evaluation and intercomparison of coupled climate models. Clim Dyn, 17(2–3): 83–106

Lau K M, Wu H T, Kim K M (2012). A robust response of precipitation to global warming from CMIP5 models. NASA, http://ntrs.nasa.gov/search.jsp?R = 20120015974

Lee J Y, Wang B (2014). Future change of global monsoon in the CMIP5. Clim Dyn, 42(1–2): 101–119

Li H, Dai A, Zhou T, Lu J (2010). Responses of East Asian summer monsoon to historical SST and atmospheric forcing during 1950–2000. Clim Dyn, 34(4): 501–514

Li Y G, He D, Hu J M, Gao J (2014). Variability of extreme precipitation over Yunnan Province, China 1960–2012. Int J Climatol, doi: 10.1002/joc.3977

Li Y H, Qing J M, Li Q, Luo W L (2012). Inter-annual and inter-decadal variations of South Asian High in summer and its influences on flood/drought over western southwest China. Journal of Southwest University (Natural Science Edition), 34(9): 71–81

Liu C L, Allan R P, Huffman G J (2012). Co-variation of temperature and precipitation in CMIP5 models and satellite observations. Geophys Res Lett, 39: L13803

Liu Y, Avissar R, Giorgi F (1996). Simulation with the regional climate model RegCM2 of extremely anomalous precipitation during the 1991 east Asian flood: an evaluation study. Journal of Geophysical Research Atmospheres, 101(D21): 26199–26215

Lu M Y, Zhu F C, Huang W Q (1987). Eigenvectors of 100hPa southern Asia high and its relationship with summer rainfall in China. Journal of Tropical Meteorology, 3(1): 125–132 (in Chinese)

Meinshausen M, Smith S J, Calvin K, Daniel J S, Kainuma M L T, Lamarque J F, Matsumoto K, Montzka S A, Raper S C B, Riahi K, Thomson A, Velders G J M, van Vuuren D P P (2011). The RCP greenhouse gas concentrations and their extensions from 1765 to 2300. Clim Change, 109(1–2): 213–241

Min S K, Park E, Kwon W T (2004). Future projections of East Asian climate change from multi-AOGCM ensembles of IPCC SRES scenario simulations. J Meteorol Soc Jpn, 82(4): 1187–1211

Nakicenovic N, Swart R (2000). Special Report on Emissions Scenarios: A Special Report of Working group III of the Intergovernmental Panel on Climate Change. Cambridge and New York: Cambridge University Press, 599

Polade S D, Gershunov A, Cayan D R, Dettinger M D, Pierce D W (2013). Natural climate variability and teleconnections to precipitation over the Pacific - North American region in CMIP3 and CMIP5 models. Geophys Res Lett, 40(10): 2296–2301

Qi D M, Zhou C Y, Li Y Q, Chen Y R (2012). Cause analysis of climate changes in southwest China. Plateau and Mountain Meteorology Research, 32(1): 35–42 (in Chinese)

Qian W H, Zhang Z J (2012). Planetary-scale and regional-scale anomaly signals for persistent drought events over Southwest China. Chin J Geophys, 55(5): 1462–1471 (in Chinese)

Rayner N A, Parker D E, Horton E B, Folland C K, Alexander L V, Rowell D P, Kent E C, Kaplan A (2003). Global analyses of sea surface temperature, sea ice, and night marine air temperature since the late nineteenth century. J Geophys Res, D, Atmospheres, 108 (D14): 4407

Sato T, Kimura F, Kitoh A (2007). Projection of global warming onto regional precipitation over Mongolia using a regional climate model. J Hydrol (Amst), 333(1): 144–154

Song J, Yang H, Li C Y (2011). A further study of causes of the severe drought in Yunnan province during the 2009/2010 winter. Chinese Journal of Atmospheric Sciences, 35(6): 1009–1019 (in Chinese)

Song Y, Qiao F, Song Z, Jiang C (2013). Water vapor transport and cross-equatorial flow over the Asian-Australia monsoon region simulated by CMIP5 climate models. Adv Atmos Sci, 30(3): 726–738

Taylor K E, Stouffer B J, Meehl G A (2012). An overview of CMIP5 and the experiment design. Bull Am Meteorol Soc, 93(4): 485–498

Tebaldi C, Knutti R (2007). The use of the multimodel ensemble in probabilistic climate projections. Philosophical Transactions of the Royal Society, 365(1857): 2053–2075

van Vuuren D P, Den Elzen M G, Lucas P L, Eickhout B, Strengers B J, van Ruijven B, Wonink S, van Houdt R (2007). Stabilizing greenhouse gas concentrations at low levels: an assessment of reduction strategies and costs. Clim Change, 81(2): 119–159

Wang B, Wu R, Fu X (2000). Pacific-east Asian teleconnection: how does ENSO affect east Asian climate? J Clim, 13(9): 1517–1536

Wang H J (2001). The weakening of the Asian monsoon circulation after the end of 1970's. Adv Atmos Sci, 18(3): 376–386

Wang H J, Fan K (2013). Recent changes in the East Asian monsoon. Chinese Journal of Atmospheric Sciences, 37(2): 313–318 (in

Chinese)

Wang T, Hamann A, Spittlehouse D L, Aitken S N (2006). Development of scale‐free climate data for Western Canada for use in resource management. Int J Climatol, 26(3): 383–397

Watanabe M (2004). Asian jet waveguide and a downstream extension of the North Atlantic Oscillation. J Clim, 17(24): 4674–4691

Wei W, Zhang R, Wen M, Rong X Y, Li T (2013). Impact of Indian summer monsoon on the South Asian High and its influence on summer rainfall over China. Clim Dyn, 43(5–6): 1257–1269

Wild M, Schmucki E (2011). Assessment of global dimming and brightening in IPCC-AR4/CMIP3 models and ERA40. Clim Dyn, 37 (7–8): 1671–1688

Xiao Z N, Yan H M, Li C Y (2002). The relationship between Indian ocean SSTA dipole index and the precipitation and temperature over China. Journal of Tropical Meteorology, 18(4): 335–344 (in Chinese)

Xu C H, Xu Y (2012). The projection of temperature and precipitation over China under RCP scenarios using a CMIP5 multi-model ensemble. Atmospheric and Oceanic Science Letters, 5(6): 527–533

Yang H, Song J, Yan H M, Li C Y (2012). Cause of the severe drought in Yunnan Province during winter of 2009 to 2010. Climatic and Environmental Research (in Chinese), 17 (3): 315–326

Yang J, Liu Q, Xie S P, Liu Z, Wu L (2007). Impact of the Indian Ocean SST basin mode on the Asian summer monsoon. Geophys Res Lett, 34(2): L02708

Zhang L, Dong M, Wu T (2011). Changes in precipitation extremes over Eastern China simulated by the Beijing Climate Center Climate System Model (BCC-CSM1. 0). Clim Res, 50(2): 227–245

Zhang X N (2012). Research on interannual variability of air-sea interaction over Indo-pacific warm pool region and its relationship with low-latitude plateau summer precipitation anomaly. Ph. D. Dissertation for Ph.D Degree. Yunnan: Yunnan University (in Chinese)

Zhou X H, Xiao Z N (2014). Climate projection over Yunnan Province and the surrounding regions based on CMIP5 data. Climatic and Environmental Research, 19 (5): 601–613 (in Chinese)